New Thermochromic Liquid–Crystalline Polymer: Synthesis and Phase Behavior

Ying Wang, Jian-She Hu, Bao-Yan Zhang, Tong-Ying Jiang

Center for Molecular Science and Engineering, Northeastern University, Shenyang 110004, People's Republic of China

Received 24 November 2004; accepted 11 January 2005
DOI 10.1002/app.22040
Published online in Wiley InterScience (www.interscience.wiley.com).

ABSTRACT: A series of new thermochromic side-chain liquid–crystalline polymers were prepared. The chemical structures of the resulting monomers and polymers were characterized by element analyses, FTIR, ^{1}H-NMR, and ^{13}C-NMR. Their mesogenic properties were investigated by differential scanning calorimetry, thermogravimetric analyses, polarizing optical microscopy, and X-ray diffraction measurements. The influence of the content of dye groups on phase behavior of the polymers was discussed. The polymers $\mathbf{P_1}$–$\mathbf{P_3}$ showed smectic phase, and $\mathbf{P_4}$–$\mathbf{P_7}$ revealed cholesteric phase. The polymers containing less than 30 mol % of the dye groups showed good solubility, reversible phase transition, wider mesophase temperature ranges, and higher thermal stability. Experimental results demonstrated that the clearing temperature and mesophase temperature ranges decreased with increasing the concentration of the dye groups. © 2005 Wiley Periodicals, Inc. J Appl Polym Sci 98: 329–335, 2005

Key words: thermochromic; smectic phase; cholesteric phase; liquid– crystalline polymers (LCP); synthesis; phase behavior

INTRODUCTION

Today, liquid–crystalline materials are directed toward the development of multifunctional structures. Indeed, liquid –rystalline polymers (LCPs) containing mesogenic and dye groups have attracted considerable interest in obtaining new materials with desirable properties.[1–4] Recently, much attention has been paid to reversible and irreversible photochromic or thermochromic LCPs for potential applications such as data storage materials.[5–10] Malachite green lactone is a well-known organic compound with thermochromic properties and it can be reversibly converted to colored dyes in the presence of a chromogenic agent and solvent on heating or cooling cycles.

In the past decade, photochromic LCP systems containing spiropyran, spirooxazine, and azobenzene derivatives have been widely reported.[11–19] As far as we know, no reports have been observed about malachite green lactone derivatives for thermochromic LCP systems. It has therefore been necessary to synthesize various kinds of thermochromic LCPs to explore their potential applications.

In this study, new side-chain LCPs containing cholesteryl 4-allyloxybenzoate and malachite green lactone 5-(undec-10-en-1-ylamidate) were synthesized. The structures and LC properties of the monomers and polymers obtained were characterized with element analyses, FTIR, ^{1}H-NMR, and ^{13}C-NMR, polarizing optical microscopy (POM), differential scanning calorimetry (DSC), thermogravimetric analysis (TGA), and X-ray diffraction (XRD) measurements. The influence of the dye groups on phase behavior of the polymers was discussed.

Correspondence to: B.-Y. Zhang (baoyanzhang@hotmail.com).

Journal of Applied Polymer Science, Vol. 98, 329–335 (2005)

EXPERIMENTAL

Materials

Polymethylhydrosiloxane (PMHS, $\bar{M}_n$ = 700–800) was purchased from Jilin Chemical Industry Co. Cholesterol was purchased from Henan Xiayi Medical Co. 5-Aminomalachite green lactone was obtained from Shenyang Chemical Engineering Research Institute. Toluene used in the hydrosilylation reaction was first refluxed over sodium and then distilled under nitrogen. All other solvents and reagents were purified by standard methods.

Measurements

The element analyses were carried out by using a Elementar Vario EL III (Elementar, Germany). FT-IR spectra were measured on a Perkin–Elmer Spectrum One (B) spectrometer (Perkin–Elmer, Foster City, CA). ^{1}H-NMR spectra (300 MHz) and ^{13}C-NMR (75.4 MHz) spectra were obtained with a Varian Gemini 300 spectrometer (Varian Associates, Palo Alto, CA). Phase transition temperatures and thermodynamic parame-

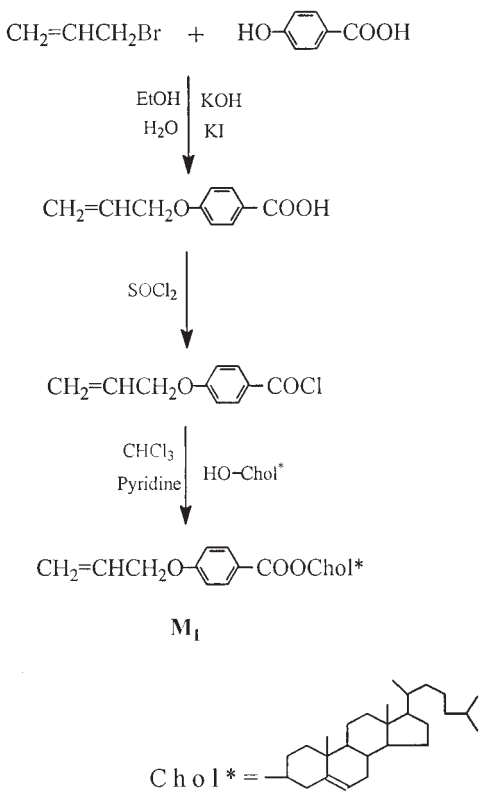

Scheme 1 Synthetic route of cholesteric monomer.

ters were determined by using a Netzsch DSC 204 (Netzsch, Germany) equipped with a liquid nitrogen cooling system. The heating and cooling rates were 10°C min^{-1}. The phase transition temperatures were collected during the second heating. The thermal stability of the polymers under atmosphere was measured with a Netzsch TGA 209C thermograrimetric analyzer. A Leica DMRX (Leica, Germany) polarizing optical microscope equipped with a Linkam THMSE-600 (Linkam, England) cool and hot stage was used to observe phase transition temperatures and optical textures of LC the monomers and polymers. XRD measurements were performed with nickel-filtered Cu-Kα (λ = 0.1542 nm) radiation with a DMAX-3A Rigaku (Rigaku, Japan) powder diffractometer. The scattering vector lies in the horizontal direction and its length is defined as $q = 4\pi\sin\theta / \lambda$.

Monomer synthesis

The synthesis of olefinic monomers is shown in Schemes 1 and 2. 5-Aminomalachite green lactone was obtained from Shenyang Chemical Engineering Research Institute.

Cholesteryl 4-allyloxybenzoate (M_1)

Cholesteryl 4-allyloxybenzoate was prepared according to similar procedures previously reported:[20] yield 72.3%, m.p. 107°C.

Elem. Anal. Calcd. for $C_{37}H_{54}O_3$: C, 81.27%; H, 9.95%. Found: C, 81.19%; H, 10.18%.

IR (KBr): 3051 (=C–H); 2965, 2854 (–CH_3, –CH_2–); 1735 (C=O); 1634 (C=C); 1606, 1508 cm^{-1} (Ar–).

^{1}H-NMR ($CDCl_3$, TMS, δ, ppm): 0.67–2.03 (m, 43H, cholesteryl-*H*); 4.47 (t, 2H, -OCH_2–); 4.69–5.18 (m, 2H, CH_2 = CH–); 5.36 (m, 1H, =C*H*– in cholesteryl); 6.02 (m, 1H, CH_2=C*H*–); 6.92–7.98 (m, 4H, Ar–*H*).

^{13}C-NMR ($CDCl_3$, TMS, δ, ppm): 20.1, 20.3, 18.6, 21.9 (CH_3); 32.3, 32.1, 39.5, 29.8, 20.7, 31.8, 21.5, 21.8, 36.1, 25.2 (methylene–C); 75.2, 42.7, 30.1, 46.7, 48.0, 29.4, 28.7 (tert. C in cholesteryl); 113.8, 130.9 (aromatic tert. C); 39.1, 40.2 (quart. C in cholesteryl); 122.6, 166.5 (aromatic quart. C); 75.4 (–CH_2O–); 115.3 (CH_2=); 137.3 (=CH–); 122.5 (=CH– in cholesteryl); 149.2 (>C = in cholesteryl); 166.8 (C=O).

Malachite green lactone 5-(10-undecen-1-ylamidate) (M_2)

22.3g (0.11 mol) of undecenyl acid chloride was added dropwise to a cold solution of 38.8g (0.1 mol) of 5-aminomalachite green lactone in 10 mL of pyridine and 200 mL of dry tetrahydrofuran (THF). The reaction mixture was heated to reflux for 7 h. The saturated sodium carbonate and toluene was added to the mixture in turn. After the organic layer was separated by extraction, the crude product was obtained by distillation under reduce pressure, dried at vacuum, and then recrystallized from toluene/ethyl acetate (2 : 1): yield 30 g (52.3%).

Elem. Anal. Calcd. for $C_{35}H_{43}N_3O_3$: C, 75.92%; H, 7.83%; N, 7.59%. Found: C, 74.83%; H, 8.05%; N, 7.47%.

IR (KBr): 3464 (–NH–); 2924, 2852 (–CH_3, –CH_2–); 1762, 1735 (C=O); 1611, 1521 cm^{-1} (Ar–).

^{1}H-NMR ($CDCl_3$, TMS), δ = 1.29–2.36 [m, 28H, –(CH_2)$_8$–, –CH_3]; 4.90–4.95 (m, 3H, –N*H*–; CH_2 =

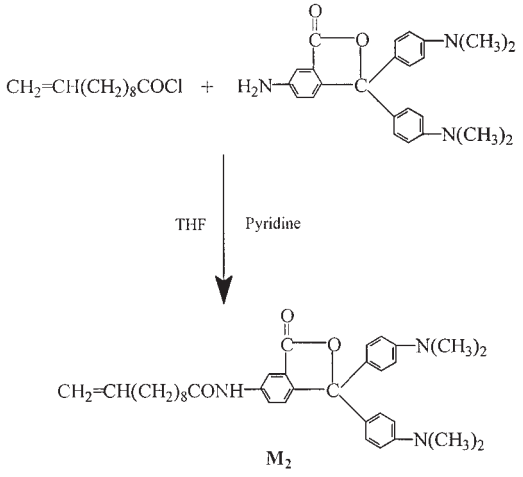

Scheme 2 Synthetic route of dye monomer.

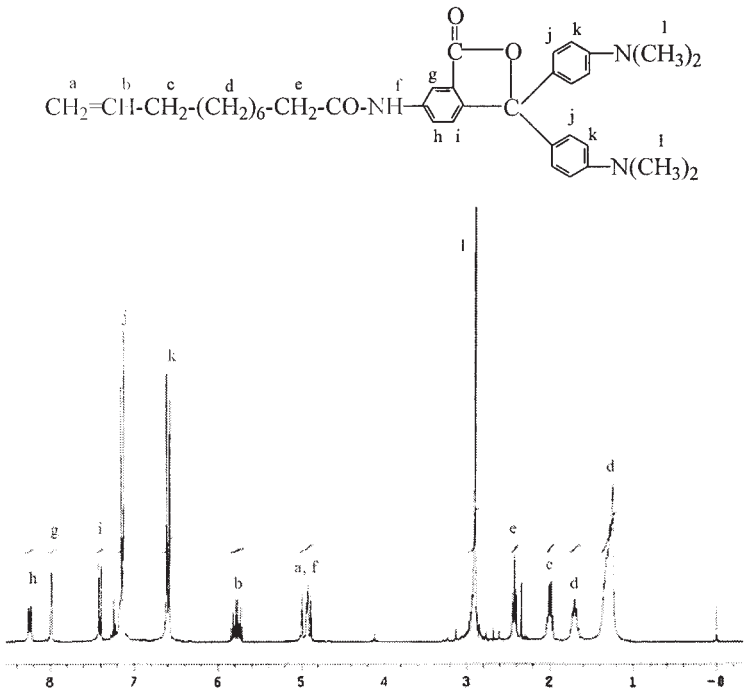

Figure 1 ^{1}H-NMR spectra of $\mathbf{M_2}$.

CH–); 5.88 (m, 1H, CH_2 = C*H*–); 6.63–8.22 (m, 11H, Ar–*H*).

^{13}C-NMR ($CDCl_3$, TMS, δ, ppm): 24.1, 28.5, 29.5, 29.9, 31.0, 33.1 (methylene–C); 43.1 (CH_3); 96.2, 111.4, 116.1, 119.3, 126.8, 128.3 (tert. C); 113.1 (CH_2=); 139.3 (=CH–); 127.3, 132.2, 137.6, 141.4, 146.7 (quart. C); 166.8, 172.2 (C=O).

Polymer synthesis

The polymers $\mathbf{P_1}$–$\mathbf{P_{10}}$ were synthesized by equivalent methods. For the synthesis of $\mathbf{P_4}$, the monomers $\mathbf{M_1}$, $\mathbf{M_2}$, and PMHS (feed ratios see Table I) were dissolved in freshly distilled toluene. The mixture was heated to 65°C under nitrogen and anhydrous conditions, and then 2 mL of THF solution of hexachloroplatinate(IV) catalyst (5 mg/mL) was injected with a syringe. The progress of the hydrosilylation reaction, monitored from the Si–H stretch intensity, went to completion within 40 h as indicated by IR. After the solvent was removed, the crude polymer was purified by precipitation in toluene with excess methanol and then dried under vacuum.

IR (KBr): 2946–2814 (–CH_3, –CH_2–); 1719 (C=O); 1600, 1501 (Ar–); 1121–1006 cm^{-1} (Si–O–Si).

RESULTS AND DISCUSSION

Syntheses

The synthetic routes for the target monomers are shown in Schemes 1 and 2. $\mathbf{M_1}$ was prepared according to the similar procedures previously reported by Hu et al.[20] $\mathbf{M_2}$ was obtained through undecenyl acid chloride reacted with 5-aminomalachite green lactone in THF in the presence of pyridine. IR spectra of $\mathbf{M_2}$ showed characteristic bands at 1762, 1735, and 1611–1521 cm^{-1} attributed to ester C=O and aromatic C=C stretching bands. ^{1}H-NMR spectra of $\mathbf{M_2}$ are shown in Figure 1. ^{1}H-NMR spectra of $\mathbf{M_2}$ showed multiplets at 1.29–2.36, 4.90–5.88, and 6.63–8.22 ppm corresponding to methyl and methylene protons, olefinic protons, and aromatic protons, respectively.

The structures of the target polymers are described in Scheme 3. The polysiloxanes were prepared by hydrosilylation reaction between Si–H groups of PMHS and olefinic C=C of $\mathbf{M_1}$ and $\mathbf{M_2}$ in toluene, using hexachloroplatinate(IV) as catalyst at 65°C. The IR spectra of the polymers showed the complete dis-

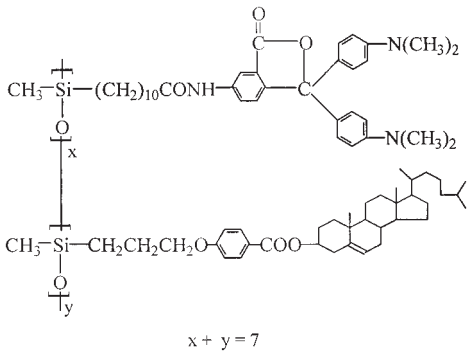

Scheme 3 Structure of copolymers.

TABLE I
Polymerization and Solubility

Polymer	Feed (mmol)				Solubility[b]	
	$\mathbf{M_1}$	$\mathbf{M_2}$	$\mathbf{M_2}$[a] (mol %)	Yield (%)	Toluene	DMSO
$\mathbf{P_1}$	7.00	0.00	0	83	+	+
$\mathbf{P_2}$	6.65	0.35	5	85	+	+
$\mathbf{P_3}$	6.30	0.70	10	85	+	+
$\mathbf{P_4}$	5.95	1.05	15	78	+	+
$\mathbf{P_5}$	5.60	1.40	20	75	+	+
$\mathbf{P_6}$	5.25	1.75	25	74	+	+
$\mathbf{P_7}$	4.90	2.10	30	76	+	+
$\mathbf{P_8}$	4.55	2.45	35	70	+	+
$\mathbf{P_9}$	—	2.45	—	72	—	—
$\mathbf{P_{10}}$	—	7.00	—	75	—	—

[a] Molar fraction of $\mathbf{M_2}$ based on ($\mathbf{M_1}$ + $\mathbf{M_2}$).
[b] +, soluble; —, insoluble.

appearance of the Si–H stretching band at 2166 cm^{-1}. Characteristic Si–O–Si stretching bands appeared at 1200–1000 cm^{-1}. In addition, the absorption bands of ester C=O and aromatic still existed. The polymerization, yields, and solubility of the polymers are summarized in Table I. The copolymers $\mathbf{P_2}$–$\mathbf{P_8}$ containing both mesogenic and dye groups were in the form of powder and found to be well soluble in toluene, xylene, dimethyl sulfoxide (DMSO), and *N*,*N*-dimethylformamide (DMF). However, homopolymers $\mathbf{P_9}$ to $\mathbf{P_{10}}$ only containing dye groups were insoluble in hot toluene, xylene, DMSO, and DMF. This indicates that the solubility of the polymers was improved when the mesogenic groups were incorporated into the polymers because of the changes of chemical structures.

Texture analysis

The optical textures and phase transition temperatures of the monomers and polymers are observed by POM with hot stage. Their phase transition temperatures obtained from DSC determination were consistent with POM observation results.

POM observation results showed that $\mathbf{M_1}$ exhibited cholesteric oily-streak texture and focal–conic texture on heating and cooling cycles. $\mathbf{M_2}$ revealed no mesomorphism and texture. Photomicrographs of $\mathbf{M_1}$ are shown in Figure 2(a) and (b). The polymers $\mathbf{P_1}$–$\mathbf{P_3}$ exhibited smectic fan-shaped texture, and the expected cholesteric phase did not appear, the reason for which is that the polymer chains hinder the formation of the helical supermolecular structure of the mesogens. $\mathbf{P_4}$–$\mathbf{P_7}$ exhibited cholesteric oily-streak texture, and $\mathbf{P_8}$ showed no texture. This indicates that the copolymer composition not only affects the phase transition temperatures of LCPs but also the mesogenic properties. Photomicrographs of $\mathbf{P_2}$ and $\mathbf{P_5}$ as examples are shown in Figure 3(a) and (b).

Thermal analysis

The thermal properties of the polymers $\mathbf{P_1}$–$\mathbf{P_8}$ were determined with DSC. The corresponding phase transition temperatures, obtained during the second heating cycles, are summarized in Table II. Representative DSC curves of the copolymers are presented in Figure 4.

For $\mathbf{P_1}$–$\mathbf{P_7}$, a glass transition at low temperature and a LC to isotropic transition at high temperature ap-

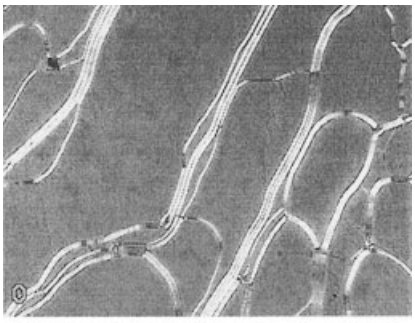

(a)

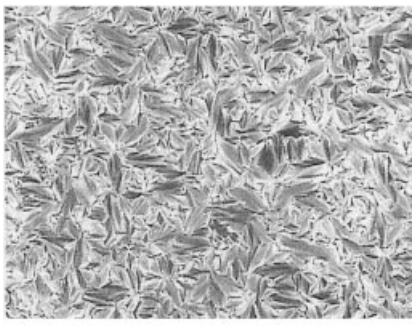

(b)

Figure 2 Optical textures of $\mathbf{M_1}$ (200×): (a) oily-streak texture on heating to 219°C; (b) focal–conic texture on cooling to 212°C.

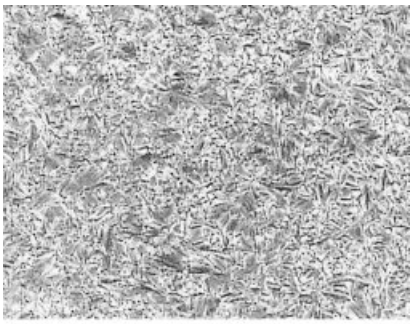

(a)

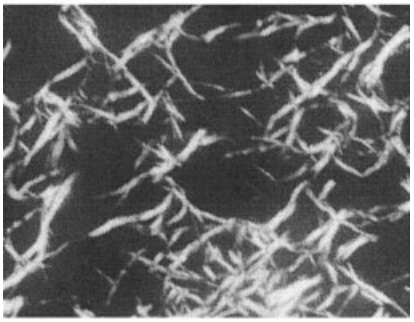

(b)

Figure 3 Optical textures of polymers (200×): (a) fan-shaped texture of $\mathbf{P_2}$ at 234°C; (b) oily-streak texture of $\mathbf{P_5}$ at 221°C.

peared on DSC curves. According to Table II, low concentration of the dye groups did not significantly influence the phase behavior of the LCPs; reversible phase transitions were observed. In contrast, high content of the dye groups had a strong influence on the phase behavior; it could cause the mesophase to disappear due to depression of mesogenic orientational order. Consequently, the DSC curve of $\mathbf{P_8}$ only showed a glass transition; no mesophase to isotropic phase transition was seen. Above all, the phase transitions are reversible and do not change on repeated heating and cooling cycles.

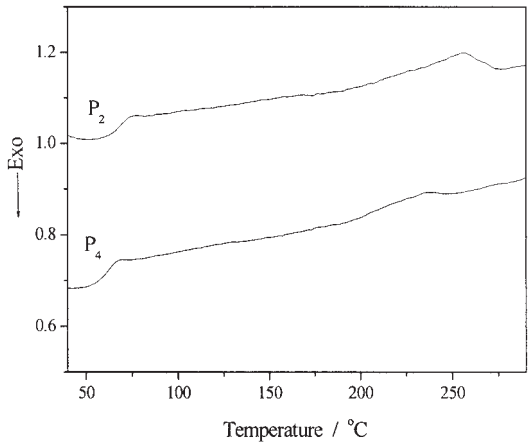

Figure 4 DSC thermograms of $\mathbf{P_2}$ and $\mathbf{P_4}$.

The glass transition temperature (T_g) is an important parameter in connection with structures and properties. For side-chain LCPs, T_g is influenced by the nature of the polymer backbone, the rigidity of the mesogenic groups, the length of the flexible spacer, and the copolymer composition. In general, bulky side groups impose additional constraints on the motion of chain segments due to the steric hindrance effect and cause an increase in T_g. However, the effect may be small for low content of side groups, and T_g is also affected by the length of the flexible spacer of side chains similar to the plasticization effect. Figure 5 shows the effect of the content of dye groups on the phase transition temperatures of the polymers. T_g decreased from 71.6°C of $\mathbf{P_1}$ to 62.9°C of $\mathbf{P_5}$ when the content of the dye side groups increased from 0 to 20 mol %. The reason for which is 1) the plasticization effect of the flexible spacer of side groups increases and 2) the content of bulky cholesteryl groups decreases though the content of bulky dye groups increases. However, T_g of the copolymers began to in-

TABLE II
Thermal Properties of Polymers

Polymer	DSC			Weight loss (%)				
	T_g (°C)	T_i (°C)	ΔT[a]	300°C	400°C	500°C	T_d[b] (°C)	LC phase[c]
$\mathbf{P_1}$	71.6	278.3	206.7	0.9	60.8	73.5	331.2	S_A
$\mathbf{P_2}$	67.8	257.1	189.3	0.5	59.9	74.7	335.7	S_A
$\mathbf{P_3}$	64.2	240.8	176.6	0.7	60.7	73.8	331.3	S_A
$\mathbf{P_4}$	63.8	236.2	172.4	0.6	53.5	69.5	333.5	Ch
$\mathbf{P_5}$	62.9	225.5	162.6	0.9	56.9	72.5	334.4	Ch
$\mathbf{P_6}$	66.7	221.4	154.7	0.6	55.9	72.0	334.1	Ch
$\mathbf{P_7}$	68.4	210.6	142.2	0.9	51.1	69.1	336.3	Ch
$\mathbf{P_8}$	70.6	—	—	0.5	55.5	70.2	332.3	—

[a] Mesophase temperature ranges (T_i–T_g).
[b] Temperature at which 5% weight loss occurred.
[c] S_A, smectic A; Ch, cholesteric.

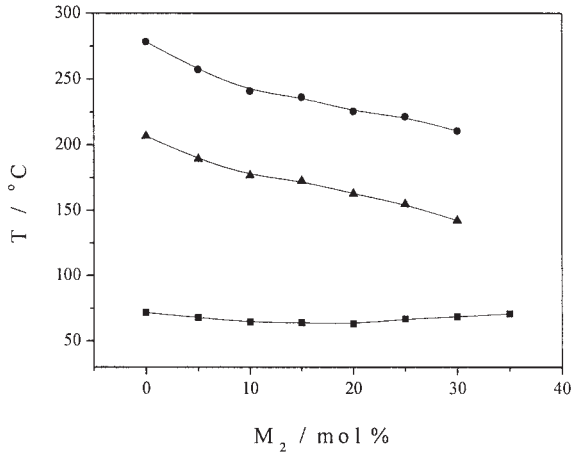

Figure 5 Effect of $\mathbf{M_2}$ content on phase transition temperatures of polymers. ([squlf]) T_g, ([circf]) T_i, ([trif]) ΔT.

crease when the content of the dye side groups was greater than 20 mol %. For $\mathbf{P_5}$–$\mathbf{P_8}$, T_g increased from 62.9 to 70.6°C when the content of the dye side groups increased from 20 to 35 mol % due to the steric hindrance effect of the bulky dye groups.

The content of the dye groups not only affected T_g of the LCPs, but also the clearing temperature (T_i). Because of the diluent effect of the dye groups, it caused a decrease in T_i. According to Table II, T_i decreased from 278.3°C of $\mathbf{P_1}$ to 210.6°C of $\mathbf{P_7}$ when the content of the dye side groups increased from 0 to 30 mol %. The mesomorphic properties disappeared when the content of the dye groups was greater than 30 mol %.

TGA of the polymer was carried out in air. TGA results of the polymers are shown in Table II. Figure 6 presents TGA thermograms of $\mathbf{P_2}$ and $\mathbf{P_4}$. TGA results showed that the temperatures at which 5% weight loss occurred (T_d) were greater than 330°C for $\mathbf{P_1}$–$\mathbf{P_8}$; this indicates that the synthesized polymers possess good

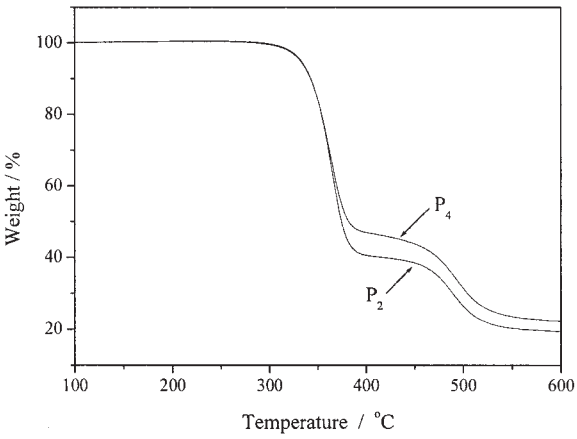

Figure 6 TGA thermograms of $\mathbf{P_2}$ and $\mathbf{P_4}$.

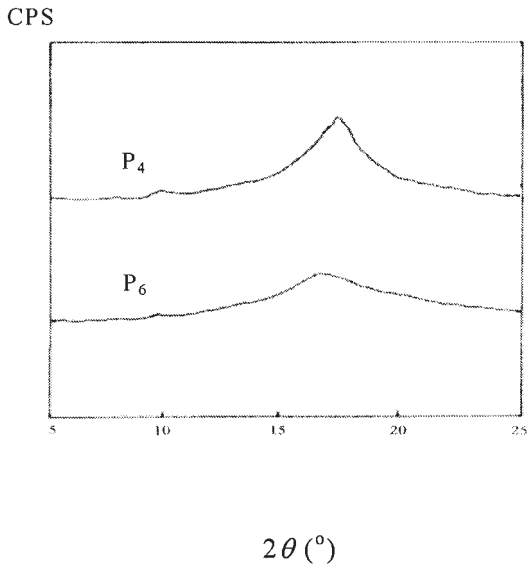

Figure 7 XRD patterns of quenched samples.

thermal and thermooxidative stability. According to Table II, the weight loss was about 70% when the temperature increased from 300 to 500°C due to the combustion of carbon and hydrogen atom in the polymers.

XRD analysis

In general, a sharp and strong peak appears at low angle ($1° < 2\theta < 4°$) in small-angle X-ray scattering (SAXS) curves for the smectic structure; no peak appears in SAXS curves and a broad peak occurred at $2\theta = 16$–$18°$ for the cholesteric structure. Representative XRD curves of quenched samples are shown in Figure 7. XRD results of quenched polymers are shown in Table III. A strong small-angle reflection associated with the smectic layers was observed at $q = 2.1$–1.8 nm^{-1}, corresponding to d-spacing of $d = 3.0$–3.4nm for $\mathbf{P_1}$–$\mathbf{P_3}$. However, a strong small-angle reflection was not observed and a broad peak appeared at $q = 11.8$–12.2 nm^{-1}, corresponding to d-spacing of $d \approx 0.52$ nm for $\mathbf{P_4}$–$\mathbf{P_7}$. Therefore, the phase structures of $\mathbf{P_1}$–$\mathbf{P_7}$ were confirmed by POM, DSC, and XRD measurements.

CONCLUSIONS

In this study, new side-chain thermochromic LCPs containing cholesteryl 4-allyloxybenzoate and malachite-green-lactone 5-(undec-10-en-1-ylamidate) side groups were synthesized and characterized. All of the obtained polymers showed high thermal stability. The polymers containing less than 30 mol % of dye groups showed reversible LC phase transition on heating and cooling cycles. For the polymers, T_g of $\mathbf{P_1}$–$\mathbf{P_5}$ de-

TABLE III
XRD Data of Polymers

Polymer	Small-angle reflections			Wide-angle reflections		
	q (nm^{-1})	d (nm)	q_1 (nm^{-1})	q_2 (nm^{-1})	d_1 (nm)	d_2 (nm)
$\mathbf{P_1}$	2.034	3.087	6.68	12.69	0.940	0.495
$\mathbf{P_2}$	1.878	3.344	6.79	12.59	0.925	0.499
$\mathbf{P_3}$	1.892	3.319	6.69	12.57	0.939	0.499
$\mathbf{P_4}$	—	—	6.70	12.15	0.937	0.515
$\mathbf{P_5}$	—	—	7.19	12.05	0.873	0.521
$\mathbf{P_6}$	—	—	6.77	11.83	0.928	0.531
$\mathbf{P_7}$	—	—	6.73	12.01	0.933	0.523

creased and T_g of $\mathbf{P_5}$–$\mathbf{P_8}$ increased; T_i and ΔT decreased with increasing the content of dye groups.

The authors are grateful to the National Natural Science Fundamental Committee of China, HI-Tech Research and development program (863) of China, Science and Technology Research Major Project of Ministry of Education of China, and Science and Technology Bureau of Shenyang for financial support of this work.

References

1. Ringsdorf, H.; Schmidt, H. W. Makromol Chem 1984, 185, 1327.
2. Cabrera, I.; Krongauz, V.; Ringsdorf, H. Mol Cryst Liq Cryst 1988, 155, 221.
3. Ono, H.; Saito, I. Jpn J Appl Phys 1999, 38, 5971.
4. Fuh, A. Y. G.; Lee, C. R.; Tsai, M. S. J Phys Rev Part B 2000, 62, 3702.
5. Petri, A.; Kummer, S.; Anneser, H.; Feiner, F.; Brauchle, C. H. Ber Bunsenges Phys Chem 1993, 97, 1281.
6. Boiko, N. I.; Kutulya, L. A.; Reznikov, A. Y.; Sergan, T. A.; Shibaev, V. P. Mol Cryst Liq Cryst 1994, 251, 311.
7. Petri, A.; Kummer, S.; Anneser, H.; Brauchle, C. H. Liq Cryst 1995, 19, 277.
8. Bobrovsky, A. Yu.; Boiko, N. I.; Shibaev, V. P. Liq Cryst 1998, 25, 679.
9. Brehmer, M.; Lub, J.; Witte, P. Adv Mater 1998, 10, 1438.
10. Witte, P.; Brehmer, M.; Lub, J. J. Mater Chem 1999, 9, 2087.
11. Shragina, L.; Buchholtz, F.; Yitzchaik, S.; Krongauz, V. Liq Cryst 1990, 7, 643.
12. Yitzchaik, S.; Ratner, J.; Buchholtz, F; Krongauz, V. Liq Cryst 1990, 8, 677.
13. Natarajan, L. V.; Bunning, T. J.; Kim, S. Y. Macromolecules 1994, 27, 7248.
14. Delvayx, C. S.; Houze, B. L.; Baillet, G.; Guglielmetti, R. J Photobiol A Chem 1995, 91, 223.
15. Hattori, H.; Uryu, T. Liq Cryst 1999, 26, 1085.
16. Hattori, H.; Uryu, T. J Polym Sci Part A Polym Chem 1999, 37, 3513.
17. Bobrovsky, A. Yu.; Boiko, N. I.; Shibaev, V. P. Adv Mater 1999, 11, 1025.
18. Hattori, H.; Uryu, T. J Polym Sci Part A Polym Chem 2000, 38, 877.
19. Zhi, J. G.; Zhang, B. Y.; Zang, B. L.; Shi, G. H. J Appl Polym Sci 2002, 85, 2155.
20. Hu, J. S.; Zhang, B. Y.; Jia, Y. G.; Chen, S. Macromolecules 2003, 36, 9060.